Supporting Information

Vertical van der Waals Heterojunction Diodes comprising 2D Semiconductors on 3D β-Ga_2O_3

Chloe Leblanc,[a] Dinusha H. Mudiyanselage,[b] Seunguk Song,[a] Huairuo Zhang,[c,d] Albert V. Davydov,[c] Houqiang Fu[b] and Deep Jariwala[a]

[a.] *Department of Electrical and Systems Engineering, University of Pennsylvania, Philadelphia, PA 19104, USA.*
[b.] *School of Electrical, Computer, and Energy Engineering, Arizona State University, Tempe, AZ 85287, USA.*
[c.] *Materials Science and Engineering Division, National Institute of Standards and Technology (NIST), Gaithersburg, MD 20899, USA.*
[d.] *Theiss Research, Inc., La Jolla, CA 92037, USA.*

e-mail: dmj@seas.upenn.edu

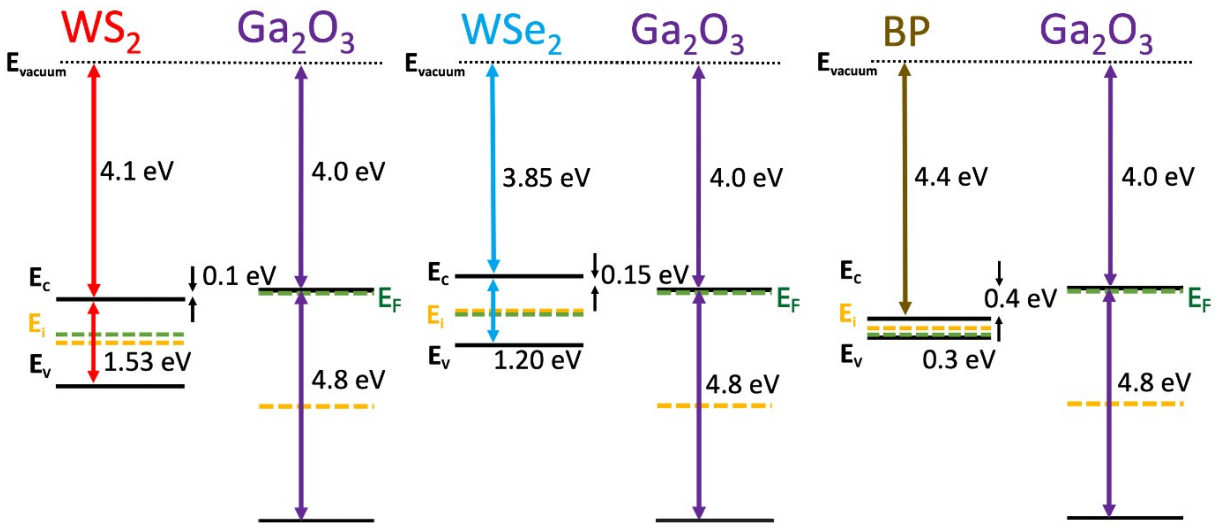

Supplementary Fig. 1 Band alignment of the three studied 2D/β-Ga_2O_3 interfaces. The alignments of the 2D matrials relative to the substrate band illustrate the p-n aspect of the junction.

Band alignment is a critical feature in heterojunctions. In straddling (type I) band diagram interfaces, one material possesses a shorter bandgap such that its conduction band minimum is lower and higher valence band minimum higher than the other material. The interface then acts as a barrier that confines electrons and holes in the first material. BP and WS_2 having smaller bandgaps and larger electron affinities than β-Ga_2O_3, BP/β-Ga_2O_3 and WS_2/β-Ga_2O_3 heterointerfaces qualify as straddling. However, the band alignment of our contacted WSe_2/β-Ga_2O_3 matches staggered (type II) interfaces, where the band minimums are offset such that one carrier type encounters an energy barrier, whereas the other faces a well at the junction.

Fig. S1 represents the resulting band diagram before contact at the interfaces between the β-Ga_2O_3 and the three 2D materials. The Fermi levels were recorded in table S1 and calculated based on the formula

$$E_F - E_i = kT\, ln(\frac{n}{n_i})$$

, where E_i is the intrinsic Fermi level located midgap, k is the Boltzmann constant, T is 298 K (room temperature), n is the electron concentration and n_i is the intrinsic density of conduction band states. The latter was found using

$$n_i = \sqrt{N_c N_v}\, exp(\frac{-E_g}{2kT})$$

Material	n_i [cm^{-3}]	$E_F - E_i$ [eV]
β-Ga_2O_3 (-201)	9.13×10^{17}	2.07
WSe_2	7.63×10^{14}	0.0069
WS_2	1.73×10^{12}	0.104
BP	1.81×10^{22}	0

Supplementary Table 1 Calculated values of intrinsic density of conduction band states n_i and Fermi level offset w.r.t. Intrinsic level (E_F-E_i) for each relevant material.

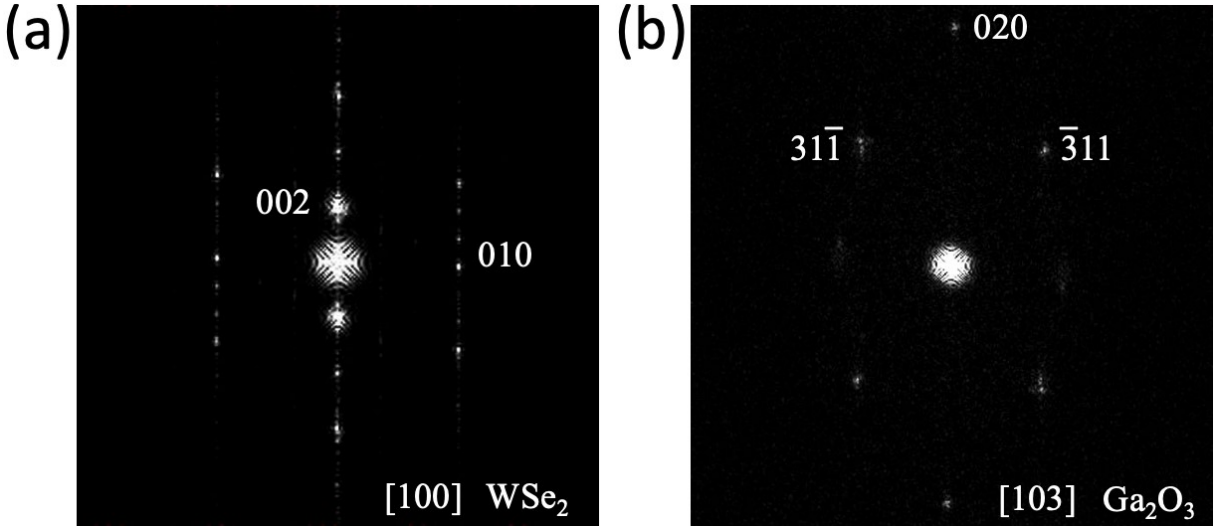

Supplementary Fig. 2 Fast-Fourier transform (FFT) images of Fig. 2(b) in the main text from the areas of (a) WSe_2 and (b) Ga_2O_3 evidencing the WSe_2 junction on the (010) oriented Ga_2O_3 substrate.

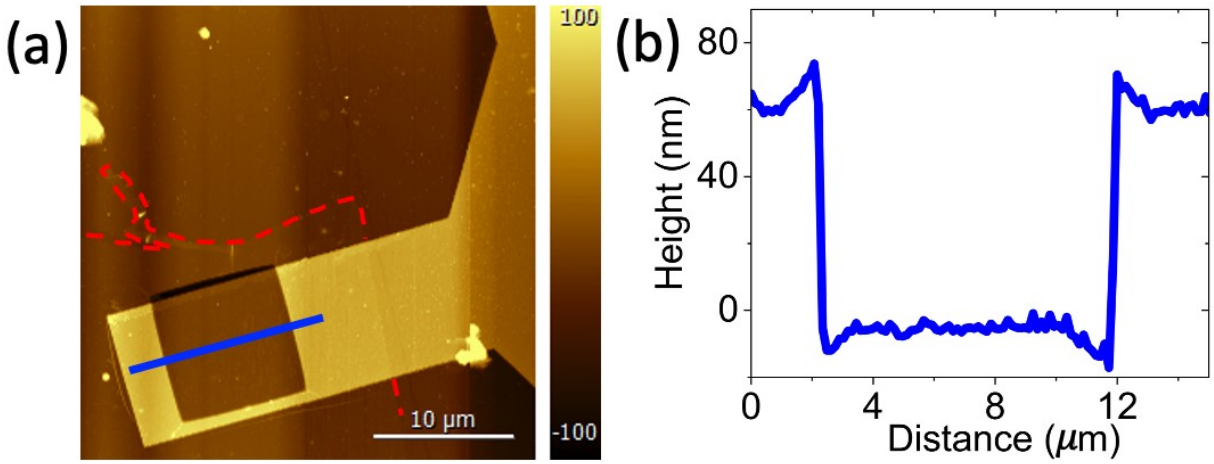

Supplementary Fig. 3 (a) Height profile of the junction presented in Fig.1(d). Red dotted line outlines the flake, and the straight blue line represents the cross-cut location. Z-scale bar units are nm. (b) Cross-cut line profile of the same junction verifies the dip in the topography of the device caused by the hole formed into the Al_2O_3.

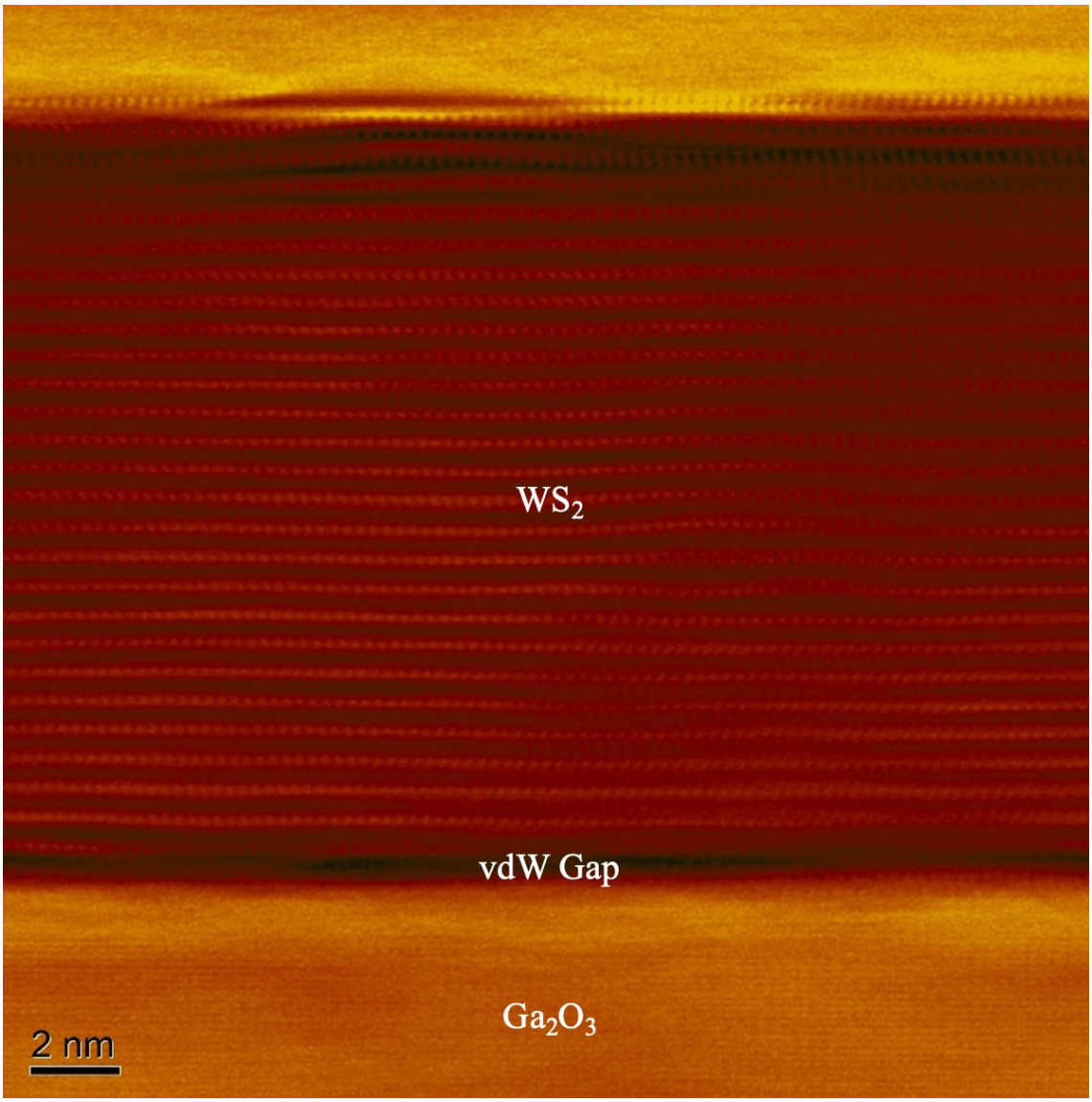

Supplementary Fig. 4 ADF-STEM characterization of a WS_2/(010) Ga_2O_3 with MoO_3/Au contacts, showing a van der Waals (vdW) gap at the WS_2/ Ga_2O_3 interface.

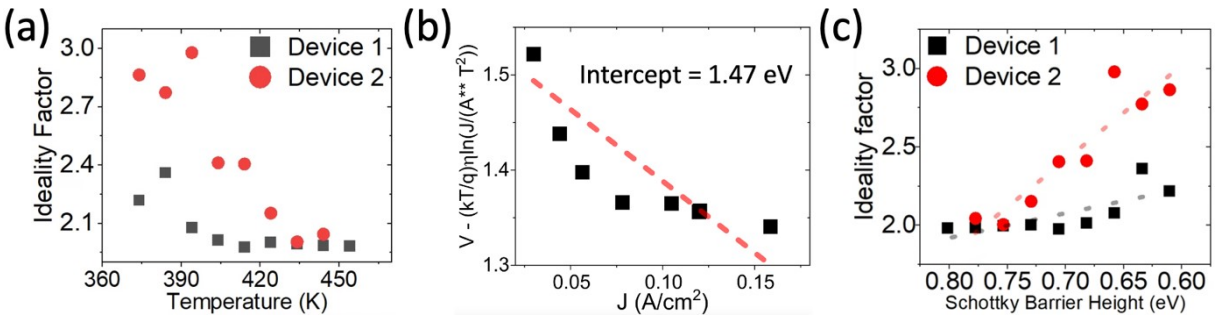

Supplementary Fig. 5 (a-b) Ideality factor dependence on temperature of two devices on (001) Ga_2O_3 orientation with WSe_2 and Ti/Au contacts. (b) Extraction of the value $n\phi_T$ at room temperature. Black squares are the experimental data points and the red line is the linear regression. A^{**} is the Richardson constant (27.6 cm^{-2} K^{-2} A) [1,2] (c) Ideality factor as a function of SBH, along with their linear regression.

In Fig.S5(b), we differentiated the thermionic emission equation and applied a linear regression to find a y-axis intercept of 1.47 eV at room temperature, from which we can deduce ϕ_T = 0.604 eV. This value is in close agreement with the predicted room-temperature SBH of Fig.S5(c).

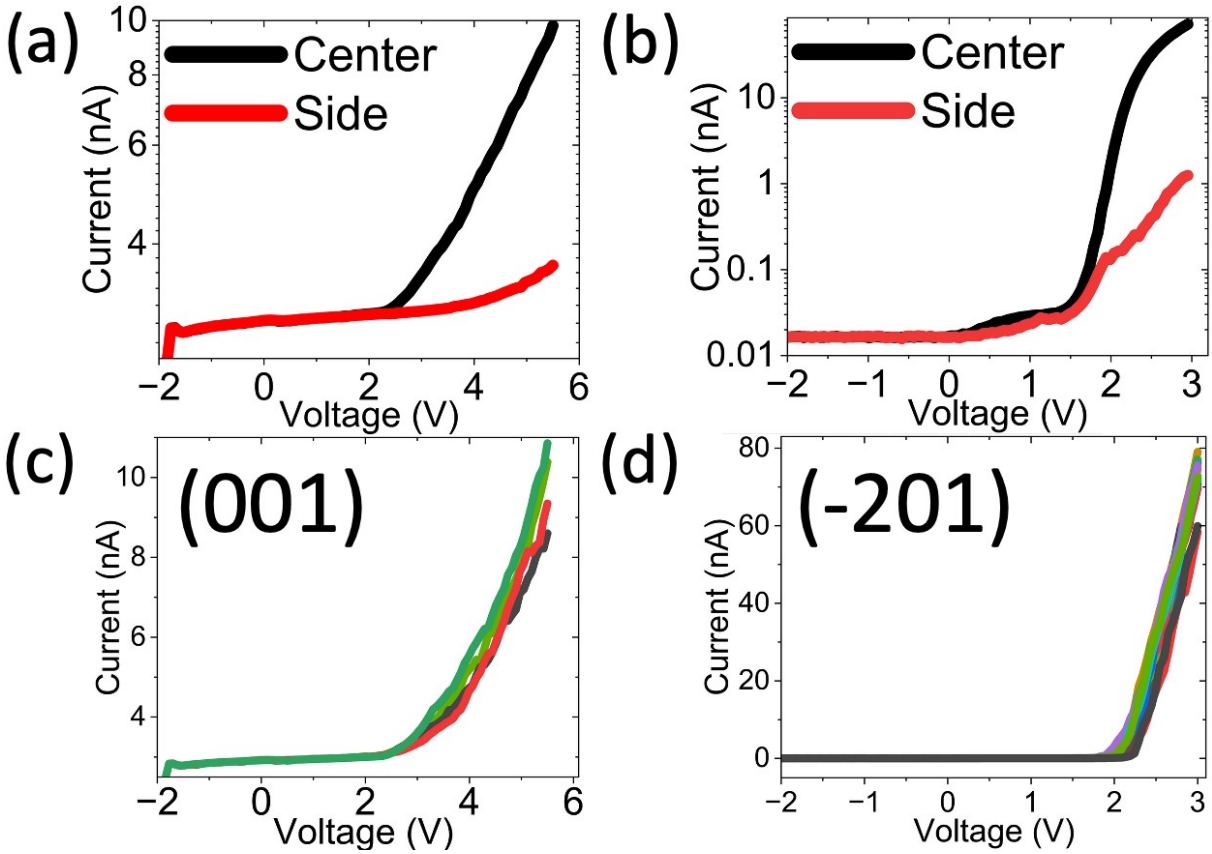

Supplementary Fig. 6 Current-voltage plots of (a,c) the (001)-oriented junction and (b,d) the (-201)-oriented junction in Fig.5. Units are nA. (a,b) Center (black) curves represent average recorded current values directly above the 2D/3D interface, and side (red) curves average recorded values around the interface. (c,d) recorded current values directly above the interface. The series resistance attributable to the measurement setup is disregarded but estimated around 10 MΩ.

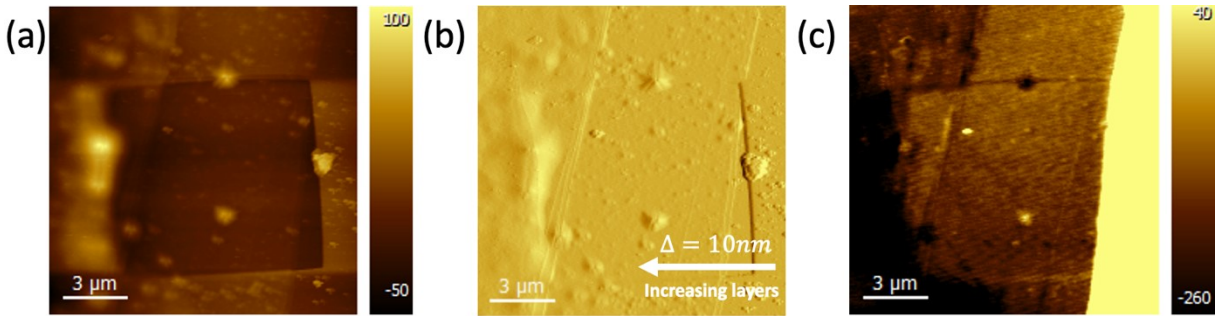

Supplementary Fig. 7 Topography (a), magnitude (b) and KPFM (c) maps of a junction located on a (-201) orientated substrate. The z-axis scale bar for the topography image in (a) is nanometers (nm). The Zz-axis scale bar for the KPFM image in (c) is millivolts (mV).

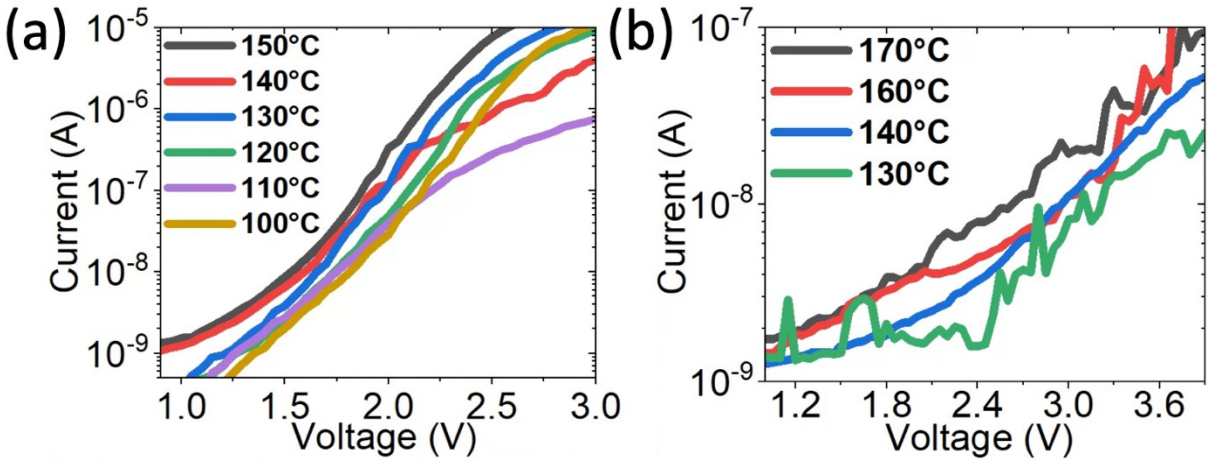

Supplementary Fig. 8 Evolution of Current-Voltage measurements of two junctions with temperature. Devices were both on a (-201) oriented sample, with WSe_2 and Ti/Au contacts.

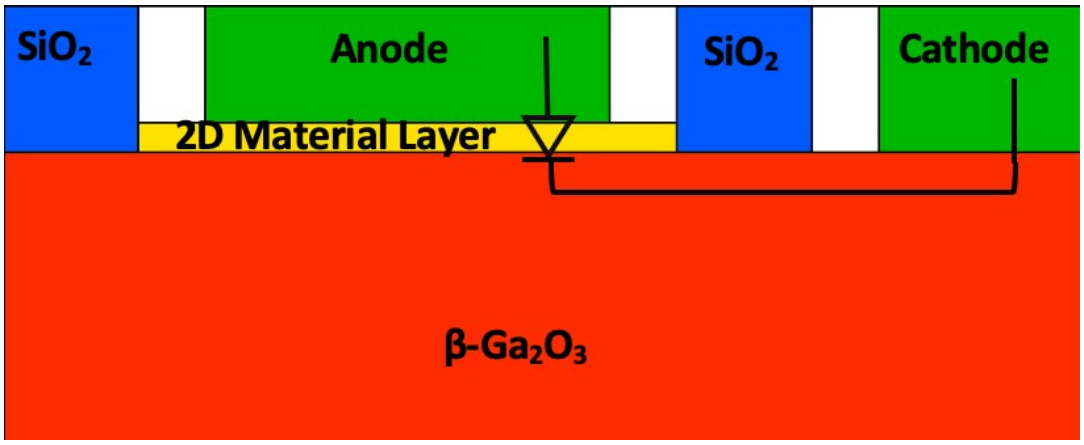

Supplementary Fig. 9 Schematics of the simulated device structure. The β-Ga_2O_3 extends further down the device and is relatively thick compared to the 2D material layer. This ensures that current spreads only near the surface of the β-Ga_2O_3 and does not have any effect on the device simulation. Even though the device seems to be in a plane, SILVACO considered 1 µm device width during the simulation.

The p-n junction between 2D material (WSe_2, WS_2, and Black Phosphorus-BP) and β-Ga_2O_3 has been implemented and simulated in SILVACO TCAD commercial software environment. The simulated device structure can be found in Fig. S8. SiO_2 has been used as a passivation layer on both sides of the 2D material. It is assumed that the thickness of the 2D layer is 20 nm, albeit the potential variation of the thickness in the real experiments. All the β-Ga_2O_3 substrates used in the experiment are highly conductive and provide a path for current conduction from the junction to the cathode as shown in Fig. S9. It should be noted that the β-Ga_2O_3 extends further down the device (not shown in Fig. S9) to account for its relative thickness compared to the 2D material layer. Furthermore, this ensures that current spreading is only near the surface of the β-Ga_2O_3 and does not have any effect on the device simulation. All the material parameters used in the simulation can be found in Table S2. The contact metal is titanium and both anode and cathode are assumed to be ohmic contacts. In the SILVACO TCAD software, the simulations used the ALTAS module. This module solves 1-D Poisson's equation based on the charge neutrality of the p-n junction for the static (bias = 0 V) and non-equilibrium or dynamic situations (bias ≠ 0). The mesh grid is dense near the p-n junction and relaxed everywhere else to achieve highly accurate calculations while reducing the computational complexity. Although the device is represented in a plane, SILVACO considered 1 µm device width during the simulation.

In SILVACO, interfaces states are considered according to the specified materials and calculate the recombination current along with the drift diffusion current. Shockley-Read-Hall (SRH) recombination and Auger recombination models are used in the simulation. More details about these models can be found in SILVACO ATLAS user manual.[4] It should be noted that we did not take into account the parasitic components mentioned in the main manuscript and assumed no parasitic resistance in the device simulations.

Supplementary Table 2: Material parameters used in the device simulations.

Materials	**Bandgap (eV)**	**Carrier Mobility ($cm^2/V·s$)**	**Density of States (cm^{-3})**	**Electron affinity (eV)**	**Relative permittivity**	**Thermal conductivity (W/cm·K)**
WS_2	1.53	44	$2.51×10^{19}$	4.1	14.6	1.15
WSe_2	1.2	142	$2.51×10^{19}$	3.85	16.0	0.41
BP	0.3	220	$2.51×10^{19}$	4.4	12.1	0.41
β-Ga_2O_3	4.9	150	$3.72×10^{18}$	4.0	10.0	0.13

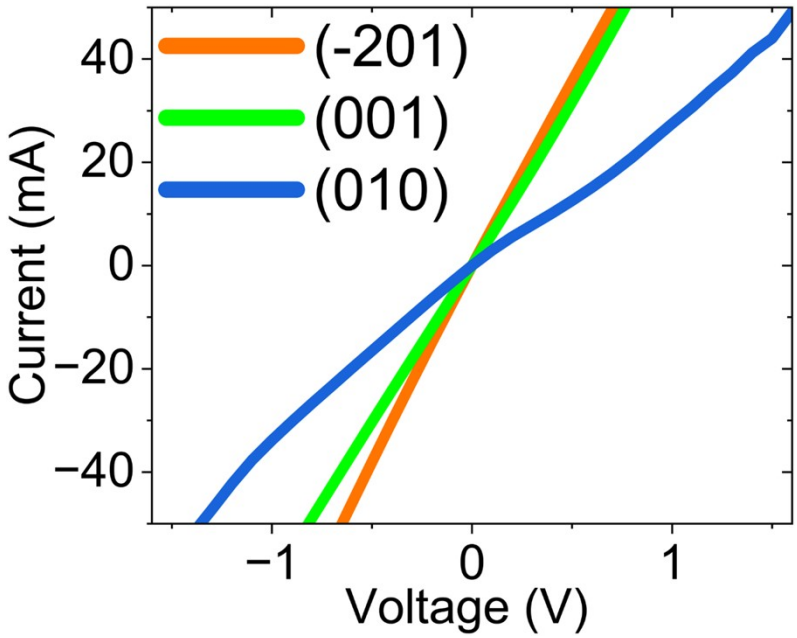

Supplementary Fig. 10 I-V measurements of the Ohmic side contacts directly onto the Ga_2O_3 substrate (see Fig. 1(a)). The stacks were deposited on the sides of the samples (see Fig. 1(a)) and consisted in Ti/Au 30/120 nm deposited by electron-beam evaporation and rapid-annealed with an RTA-600S at 500°C for 30s.

Supplementary Table 3: X-ray crystallography (XRC) of Ga_2O_3 crystal Full Width Half Length (FWHM) values. Data provided by Novel Crystal Technology, Inc.

	Ga_2O_3 Orientations					
	(-201)		**(001)**		**(010)**	
	[010] azimuth	[-10-2] azimuth	[100] azimuth	[010] azimuth	<102> azimuth	⊥ <102> azimuth
FWHM (arcsec)	<100	<100	<300	<300	<150	<150

References

1 Cheung, S. K. & Cheung, N. W. Extraction of Schottky diode parameters from forward current-voltage characteristics. *Applied Physics Letters* **49** (1986). https://doi.org:10.1063/1.97359

2 Bandyopadhyay, A. S., Saenz, G. A. & Kaul, A. B. Role of metal contacts and effect of annealing in high performance 2D WSe2 field-effect transistors. *Surface and Coatings Technology* **381** (2020).

3 Ma, D. & Chen, Y. *Organic Semiconductor Heterojunctions and Its Application in Organic Light-Emitting Diodes*

4 International, S. Atlas User's Manual Device Simulation Software (ed Silvaco Int.) (Santa Clara, 2012).

5 Jang, S. *et al.* A comparative study of wet etching and contacts on (-201) and (010) oriented B-Ga2O3. *Journal of Alloys and Compounds* **731**, 118-125 (2018).